Advances in Environmental Technology 1 (2022) 15-29

Iranian Reasearch Organization for Science and Technology (IROST)

Advances in Environmental Technology

Journal home page: https://aet.irost.ir/

Ammonium-nitrogen removal from aqueous solution using municipal green waste wood biochars

Wilson E. Ndibize[1,2,3], Md Nuralam Hossain[1,2,3*], Nan Hongyan[1,4], Muhammad Salam[1,2,3], Md. Manik Mian[5], Md. Eusuf Sarker[6], Md Rokebul Islam Shojib[7]

[1]Key Laboratory of Three Gorges Reservoir Region's Eco-Environment, Ministry of Education, Chongqing University, Chongqing, China

[2]National Center for International Research of Low-carbon and Green Buildings (Ministry of Science and Technology), Chongqing University, Chongqing, China

[3]School of Environment and Ecology, Chongqing University, Chongqing, China

[4]School of Environmental Science and Engineering, Shanghai Jiao Tong University, Shanghai, China

[5]CAS Key Laboratory of Crust-Mantle Materials and the Environments, School of Earth and Space Sciences, University of Science and Technology of China, Hefei, China

[6]Department of Environmental Science and Resource Management, Mawlana Bhashani Science and Technology University, Santosh, Tangail, Bangladesh

[7]Department of Mechanical Engineering, Chongqing University, Chongqing, China

ARTICLE INFO

Document Type:
Research Paper

Article history:
Received 11 November 2021
Received in revised form
23 February 2022
Accepted 26 February 2022

Keywords:
Ammonium nitrogen
Adsorption process
Municipal green waste
Slow pyrolysis
Wood biochar

ABSTRACT

Ammonium (NH_4^+), one of the most common types of reactive form of nitrogen in wastewater, can cause eutrophication and other environmental problems if released into waterways. This study was conducted to understand NH_4^+ adsorption mechanism of wood biochar from municipal green waste in an aqueous environment and the factors affecting NH_4^+ removal. The biochars were produced by pyrolyzing green wood waste at 300°C (WB300), 450°C (WB400), and 600°C (WB600), respectively. Biochar dosage, pH, and contact duration were studied during NH_4^+ adsorption studies to see how these variables affected the adsorption process. The adsorption process was studied using isotherms and kinetic adsorption models. The batch equilibrium and kinetic studies at 25°C, pH 7, and a contact duration of 240 minutes showed that the WB450 dosage of 0.2 g/L removed the most (NH_4^+-N) compared to WB600 and WB300. WB450 had higher affinity values and a maximum adsorption capacity of 2.34 mg/g; the 'Freundlich isotherm' model had a better fit to the equilibrium experimental data, indicating that heterogeneous sorption was preferable to monolayer sorption. Chemisorption was the dominant (NH_4^+) adsorption method, as demonstrated by the 'pseudo-second-order' kinetic model with an R^2 of 0.99. The study concludes that municipal green wood waste-based biochar can be efficient absorbents for NH_4^+ removal

*Corresponding author. Tel: + 86-23-65120750
E-mail: nuralam@cqu.edu.cn
DOI: 10.22104/AET.2022.5087.1379

from wastewater. Also, the removal efficiency can be optimized by selecting different feedstocks or the pyrolysis condition for biochar production.

1. Introduction

Urban rainfall-runoff and post-industrial pollutants have gained substantial attention owing to their impact on water quality, releasing enormous amounts of ammonium nitrogen (NH_4^+-N) into water bodies due to the urbanization process [1,2]. If high quantities of (NH_4^+-N) are discharged into the natural water supply before sufficient treatment, they can be devastating to the ecosystem [2,3]. Excessive ammonium nitrogen can produce eutrophication, the loss of oxygen, and toxins in aquatic species from rivers to lakes to other water bodies [4-6]. Ammonium nitrogen (NH_4^+-N) may be converted to nitrate (NO_3-) ions by bacteria. It is elementary for nitrate ions to infiltrate ground and surface water because they are very soluble in water and do not adhere well to soil particles [7,8]. High nitrate levels in drinking water can jeopardize human health, especially in newborns, such as blue-baby syndrome [7,9]. Drinking water with 10 mg/L nitrates has been permitted by the US Environmental Protection Agency (EPA). Up until now, there are several conventional methods, including ion exchange [10], air stripping [11], reverse osmosis [12], chemical precipitation [13], biological nitrification-denitrification treatment [14], and adsorption [15], that have been used to remove ammonium nitrogen from wastewater. Adsorption has gotten more attention from scientists than any other method because of its high level of safety, low cost, and potential use. To date, a number of adsorbents for ammonium removal have been studied and published in the literature, including zeolites [16,17], activated carbon [18,19], ceramic [20], clay [21], and biochar from plant materials [22,23]. The adsorption of nutrients and other organic contaminants from domestic, agricultural, and industrial wastewater has emerged as a promising biomaterial for biochar [24]. Pyrolysis (temperature ranges of 300 to 950℃) of biomass in a low or the absence of oxygen atmosphere under atmospheric N_2 produces biochar (BCs) that is a low-cost, stable, and environmentally acceptable solid carbon residue [25,26]. BCs play a vital role in removing diverse pollutants because of their porous structure, huge surface area, changeable surface functional group [27], and high cation exchange capacity [28]. In previous investigations, biochar from various feedstocks has been found to be effective in removing contaminants from water [29]. Nutrient molecules, particularly nitrogen and phosphorus, have lately been investigated extensively by academics. Eutrophication, which harms aquatic life, has been primarily attributed to chemicals [30]. Biochar adsorption from urban green waste has been studied, albeit only in small amounts, to remove nutrients like $NH4^+$-N from an aqueous environment. Piggery dung anaerobic digested slurry was researched for the removal of ammonium by Kizito and colleagues in 2015. [23]. Adsorption of $NH4^+$-N in the slurry was 44.64 ± 0.602 mg/g, whereas rice husk biochar adsorption was 39.8 ± 0.54 mg/g. According to Takaya et al. (2016), the impregnation of magnesium-impregnated biochar with low levels (2.1-3.6%) to high levels (66.4-70.3%) provides environmental and socio-economic advantages [31]. Furthermore, prior writers have explored the capacity of biochar to absorb nitrogen and phosphorus molecules [32,33]. According to some researchers, many nutrients, including nitrate, ammonium, and phosphate, have been found in post-adsorption biochar. For soil improvement, it can be used as a fertilizer [22,34]. As a bonus, biochar contains a lot of carbon, which may be added to the soil after adsorption to help it retain carbon [35,36]. Agricultural wastes have been used as biomass fuel since they are free and non-toxic. Agricultural waste has been utilized as a fuel for biochar production to enhance waste management and remove contaminants such as NH_4^+-N from the aquatic environment [22,23]. According to our understanding, there is a lack of information on the application of municipal green waste biochar to adsorb nutrients such as NH_4^+-N from wastewater. In this study, the wood portion from municipal green waste was selected to make biochar, a promising way to manage the green wastes in Chongqing, China. The produced biochar was further used to investigate their feasibility on the adsorption of NH_4^+-N, which has recently received

considerable attention due to its adverse impacts on the aquatic environment. The study's positive element shows that municipal green waste and water pollution may both be managed in an environmentally friendly manner. The study investigated the feasibility of slow pyrolysis to convert the wood wastes from municipal green wastes into biochar for NH_4^+-N adsorption. The following are objectives of this study: (1) determine the influence of pyrolysis temperature on biochar production; (2) To achieve equilibrium adsorption capacity, determine the influence of the starting concentration of NH_4^+-N, the effect of adsorbent dosage, the effect of initial solution pH, and the effect of contact time of NH_4^+-N onto biochar; and (3) analyze the adsorption process using isotherms and kinetics models of adsorption.

2. Materials and methods

2.1. Preparation of biochar and its characterization

The wood-based biochars were produced at the pyrolysis temperature of 300ºC (WB300), 450ºC (WB450), and 600ºC (WB600) (Figure 1). The production of the wood waste biochar was described in Lou et al. (20160) [37]. Briefly, the wood was cut to a ≤20 mm length, dried at 105℃ for 24 hours, and then pyrolyzed in a fixed bed reactor at 300℃, 450℃, and 600℃ in a nitrogen environment. The reactor was programmed with a heating rate of 5℃ min^{-1} to maintain the target temperature for two hours. The biochar obtained were allowed to cool down under nitrogen flow, then were ground and sieved to a size≤0.15 mm. According to pyrolysis temperature, the resulting biochar particles were abbreviated WB300, WB450, and WB600 and stored in an airtight desiccator for future use. The pH of the biochar samples was determined by mixing biochar in ultrapure water with a pH of 7.0, in a ratio of 1:20 (w: v), similar to Kizito et al. (2015) [23].

2.2. Materials and reagents

The following items were used in this study: analytical balance (AL104, METTLER TOLEDO instrument, Shanghai, China); the pH meter (WTW, MULTI 3410 set T, USA); water purifier system (Haiyuan company, China), measuring Flask and beakers (Kuihuap, Yangzhou Sunflower glass Instrument factory, China); a constant temperature shaker (SHZ-82, Guohua Enterprise Co., Ltd., China); centrifuge (TG16-WS, Xiangyi Company, China); UV-spectrophotometer (UV-1200, Beijing Puxi General Company, China); and Ultra-Pure (UP) water 18.25MΩ.cm (Haiyuan Company, China). HCl and NaOH solutions were used to modify the pH of the solution. Ammonium nitrogen was made from anhydrous ammonium chloride. Sodium hypochlorite, sodium nitroferricyanide, and salicylic acid were used as color reagents to react with residual ammonium nitrogen. Initial concentrations of NH_4^+-N, adsorbent dosages, initial solution pH, and contact times were studied in batch adsorption studies. Room temperature was used for all analyses (approximately 25℃).

Fig. 1. Biochar preparation: (a) Before pyrolysis, (b) after pyrolysis, (c) biochar powder after grinding and sieving and (d) biochar powder packed to store in a desiccator for future use.

2.3. NH_4^+-N adsorption experiment

Salicylate spectrophotometric method

The salicylate spectrophotometric method was used to determine the residual amount of NH_4^+-N in the filtrate; 0.1 mL of the filtrate was transferred to a color tube and diluted to 8mL with ultrapure water, followed by 1mL of salicylic acid, two drops of sodium hypochlorite, and two drops of sodium nitroferricyanide. Then, it was diluted with ultrapure water up to the 10mL mark of the color tube. The solution was left for one hour to allow the color reagents to react with the residual NH_4^+-N.

After the reaction, the color changed to bluish green as the concentration of the remaining NH_4^+-N increased in the sample. A UV-1200 spectrophotometer at 697nm, cuvette 10mm, was finally used to determine the residual amount of NH_4^+-N in a filtrate, with the ultrapure water as a reference point. The color intensity was the applicable criteria for determining the NH_4^+-N concentration using a UV spectrophotometer. The standard curve (Table S1 and Figure S1) was used to get an actual concentration of NH_4^+-N from the spectrophotometer readings. A standard curve was made by transferring 0.1 mL from each of the standard experimental initial solutions (5, 10, 20, 40, 60, and 80 mg/L) NH_4^+-N into the color tubes, followed by color reagents and ultrapure water up to 10mL mark. Then, they were left for one hour to change color for spectrophotometer determination. The obtained actual concentration of NH_4^+-N in solution was then used to find the removal percentage and equilibrium amount of NH_4^+-N adsorbed per unit mass of adsorbent by using (Eq. 1 and 2), respectively.

$$\%\ \text{Removal} = \frac{C_0 - C_e}{C_0} \times 100 \quad (1)$$

$$q_e = \frac{(C_0 - C_e)V}{W} \quad (2)$$

where C_0 and C_e (mg/L) are respectively the initial and equilibrium concentration of NH_4^+-N in solution, q_e (mg/g) is the adsorbed amount of NH_4^+-N at equilibrium, V (L) is the volume of solution used, and W (g) is the mass of biochar.

Effect of initial NH_4^+-N concentration on adsorption

In order to examine the impact of the original NH_4^+-N concentration, 0.2g/L of biochar was added to NH_4^+-N solutions containing varying concentrations of $NH4^+$-N (0, 5, 10, 20, 40, 60, and 80mg/L) with a pH adjustment of 7+0.2. It was maintained at 200 r/min. for 24 hours in a constant-temperature shaker and centrifuged for five minutes to get the supernatant. A 0.45µm syringe filter was used to remove the supernatant. In order to evaluate the remaining NH_4^+-N in the filtrate, the salicylate spectrophotometric method was used to analyze the filtrate.

Effect of contact time on adsorption

The effect of contact time on NH_4^+-N removal was studied by applying 0.2 g/L of biochar in 40 mg/L of NH_4^+-N solutions. The samples were then adjusted to pH 7 and shaken in a mechanical shaker for 15min, 30min, 45min, 1h, 2h, 3h, 4h, 8h, 12h, and 24h to determine at which time equilibrium was reached.

Effect of biochar dosage on NH_4^+-N adsorption

The effect of biochar dosage on NH_4^+-N adsorption was investigated by treating 40mL of 60mg/L NH_4^+-N in different biochar dosage (0.02, 0.05, 0.1, 0.2, 0.4, 0.8 g/L); the initial NH_4^+-N concentration of 60mg/L is typical of municipal wastewater (Bolan et al. 2004). The pH was adjusted to 7.0 for consistency, shaken for 24hr, and then the salicylate spectrophotometric method was used to analyze the filtrate.

Effect of initial pH on NH_4^+-N adsorption

0.2g of WB450 was added into seven centrifuge tubes, followed by 40 mL of 40 mg/L NH_4^+N in which its initial concentration was adjusted at a pH of 3, 4, 5, 6, 7, 8, and 9 accordingly, shaken for 24hr, centrifuged, and filtered. Then, the residual amount of NH_4^+N in the filtrate was determined by the salicylate spectrophotometric method.

2.4. Adsorption kinetics study

The adsorption of NH_4^+-N by municipal green wood biochar on ammonium nitrogen was monitored for 24 hours to estimate the time required to achieve equilibrium and the adsorption amount at equilibrium. Wood biochar was utilized to model data to understand NH_4^+-N adsorption mechanisms better using pseudo-first- and pseudo-second-order kinetic models. Equations 3 and 4 show the linearized version of the pseudo-first-order equation (Eq. 3) [38].

Pseudo-first-order model

$$\log(q_e - q_t) = \log q_e - \frac{K_1}{2.303} t \quad (3)$$

Pseudo-second-order model

$$\frac{t}{q_t} = \frac{1}{K_2 q_e^2} + \frac{1}{q_e} t \quad (4)$$

where K_1 is the pseudo-first-order rate constant (per min), K_2 is the pseudo-second-order rate constant (g/ min/mg), q_t is the amount of

ammonium nitrogen adsorbed at time t (mg/g), q_e is the adsorption capacity at equilibrium (mg/g), and t is the contact time (min). A graph of $\log (q_e - q_t)$ against t was used to obtain K_1 from the slope, and q_e from the intercept. A graph of t/q_t versus t was used to obtain K_2 from the intercept of the graph and to obtain q_e from the slope.

2.5. Adsorption isotherm Study

Isotherm models are utilized to explain adsorbate interactions with the adsorbents that are equilibrium [39]. The experimental data were analyzed using the Langmuir and Freundlich isotherm models. The adsorption isotherm models for NH_4^+-N adsorption were tested using experimental data from the influence of starting concentration (Eq. 5 and 6).

The Freundlich equation is given by

$$\log q_e = \log K_f + \frac{1}{n}\log C_e \quad (5)$$

where "C_e" is a concentration of NH_4^+-N residual at equilibrium (mg/L), "q_e" is the amount of NH_4^+-N on the biochar at equilibrium (mg/g), "q_0" is the maximum monolayer coverage capacities (mg/g), "b" = relative binding energy of the biochar (L/mg), "K_f" is the relative NH_4^+-N adsorption constant, depending on the nature of an adsorbent, and "n" is the adsorption intensity of the biochar (heterogeneity factor). The value 0.1<1/n<1 = favorable, while higher Kf= higher affinity of the adsorbent. The constants "K_f" and "n" were determined from the plot of "$\log q_e$" against "$\log C_e$" in which $\log K_f$ is the intercept and 1/n is the slope [20,21,23].

The Langmuir equation is given by:

$$\frac{C_e}{q_e} = \frac{1}{bq_0} + \frac{C_e}{q_0} \quad (6)$$

For the Langmuir model, a graph of "C_e/q_e" against "C_e" was used to determine both "q_0" and "b" at the slope (1/"q_0") and intercept (1/bq_0), respectively. To determine whether the model was favorable or not, the dimensionless separation factor (R_L) was used; this is the essential characteristic of Langmuir isotherm as expressed in Eq. 7.

$$R_L = \frac{1}{1 + bC_0} \quad (7)$$

The value of dimensionless separation factor (R_L) defines the adsorption nature, whether favorable (0<R_L< 1), unfavorable (R_L= 1), irreversible (R_L= 0), or linear (R_L= 1) [21,22,40].

3. Results and Discussion

3.1. Biochar Characteristics

The biochar yields and their pH are summarized in Table 1. The table shows that as the pyrolysis temperature increased from 300 to 600ºC, the biochar yield decreased from 53.16 wt% to 31.46 wt%. This could be due to the further decomposition occurring at higher temperatures, as described by [44,46,47]. They stated that the dehydration reaction and thermal degradation led to the release of low molecular weight compounds of liquid and gaseous state, and thus lower biochar yield as more volatiles are given out. The decrease of biochar yield as the pyrolysis temperature increased was consistent with a number of studies, including pine feedstock [48], Ferula Orientalis [49], and rice husk [47]. The biochar pH was alkaline and ranged from 7.3 to 8.1 as pyrolysis temperature increased. The increasing trend of the pH value was consistent with the previous reports that attributed the trend to the release of the acidic surface group "-COOH" and the formation of carbonates "-CO_3" as the pyrolysis temperature increased [50,51].

Table 1. Biochar yields and their pH at different pyrolysis temperatures 300ºC (WB300) and 450ºC (WB450) and 600ºC (WB600).

Biochar	Feedstock mass (g)	Biochar yield (g)	Biochar yield (%)	pH
WB300	65.01	34.56	53.16	7.25
WB450	65.04	23.84	36.65	7.83
WB600	65.03	20.45	31.45	8.10

3.2. Adsorption of NH_4^+-N

The biochar WB450 showed higher potential on isotherm adsorption compared to the other two (Table 2 and Figure 2), with the maximum adsorption capacity "qo" 2.347 mg/g (Table 4). This could be due to higher carbonization form at 450ºC than at 300C; simultaneously, the adsorption functional groups could be formed at 450 ºC. On the other hand, at the higher temperature of 600 ºC, the carbonization and more functional group formation might be less. Tian et al. (2016) [52] reported that as pyrolysis temperature increased from 400°C to 500°C, more surface areas were

created; this statement is consistent with Gai et al. (2014) that found fine-pore structures could be formed [53]. But the more rise in pyrolysis temperature could destroy some of the formed fine-pore structures [43]. Simultaneously, the higher pyrolysis temperature was reported to decrease the surface functional groups [43,54,55].

Table 2. Adsorption isotherm of NH_4^+-N onto wood biochar dosage 0.2g/L in 60mL NH_4^+-N, Temp. 25ºC, pH of 7±0.2, shaking speed 200r/min for 24h.

Biochar	C_0	C_e (mg/L)	q_e (mg/g)	C_e/q_e	Log C_e	Log q_e
WB300	5	3.2452	0.3510	9.2466	0.5112	-0.4547
	10	7.1514	0.5697	12.5527	0.8544	-0.2443
	20	15.5950	0.8810	17.7012	1.1930	-0.0550
	40	34.1947	1.1611	29.4514	1.5340	0.0649
	60	53.0950	1.3810	38.4465	1.7251	0.1402
	80	70.8534	1.8293	38.7319	1.8504	0.2623
WB450	5	3.0349	0.3930	7.7217	0.4821	-0.4056
	10	6.1899	0.7620	8.1230	0.7917	-0.1180
	20	14.6034	1.0793	13.5301	1.1645	0.0332
	40	32.3317	1.5337	21.0815	1.5096	0.1857
	60	50.9916	1.8017	28.3022	1.7075	0.2557
	80	70.2524	1.9495	36.0358	1.8467	0.2899
WB600	5	3.3654	0.3269	10.2941	0.5270	-0.4856
	10	7.9627	0.4075	19.5428	0.9011	-0.3899
	20	16.9471	0.6106	27.7559	1.2291	-0.2143
	40	35.3666	0.9267	38.1647	1.5486	-0.0331
	60	54.2368	1.1526	47.0542	1.7343	0.0617
	80	72.1154	1.5769	45.7317	1.8580	0.1978

3.2.1. Initial NH_4^+N concentration effect on adsorption

At equilibrium, adsorption (mg/g) increased as the initial concentration of NH_4^+-N was increased from 5 to 80 mg/L. In terms of the capacity to adsorb NH_4^+-N, WB450 outperformed the others, as seen in Figure 2. As the initial concentration of NH_4^+-N increased, the flow of NH_4^+-N onto the unoccupied active sites increased as well [21,23]. At low initial concentration, there was a low mass flow of ions onto the biochar's unoccupied active sites. The mass flow of NH_4^+-N onto the biochar active sites increased as the ion concentration increased. The ionic gradient between the solid and liquid phases influenced the increase of the adsorbed amount. Long et al. (2008) reported that the ionic mobility becomes less random at much higher concentrations as most active sites are occupied, so the adsorption process follows charge attraction between the adsorbent and adsorbate [19].

3.2.2. Biochar dosage effect on NH_4^+-N adsorption

As the biochar dosage increased from 0.02 to 0.8g/L, the NH_4^+-N removal efficiency increased from 4.70 to 17.62, 2.87 to 11.09, and 2.56 to 10.48% for WB450, WB300, and WB600, respectively (Figure 3). Such increases in the NH_4^+-N removal efficiency may be caused by an increase in the total adsorptive surface, resulting in the increased availability of adsorptive sites [24]. The total amount of NH_4^+-N removed or the removal efficiency can be expected to continuously increase as the biochar dosage increases until the adsorption sites are saturated [68]. However, NH_4^+-N adsorption of WB450 increased from 2.81 to 10.57 mg N/g as the application rate increased from 0.02 to 0.8g/L (Figure 3). For WB450, the

increase in NH_4^+ adsorption with an initial increase in biochar dosage may be attributed to its low surface functional groups and thus low adsorption sites and adsorption capacity compared to the other two biochar. The adsorbate to adsorption site ratio for WB450 may not have decreased as much as WB300 and WB600. However, as more biochar was added, the number of adsorption sites increased, eventually resulting in fewer NH_4^+ ions diffusing onto the biochar surface, decreasing NH_4^+ adsorption per unit mass of biochar. Possible aggregation of biochar particles under higher biochar dosage may have reduced the adsorption capacity [23]; also, the same effect using other biochar [23], ion exchange resins [56], zeolites [17,57], and activated carbon have all shown comparable trends in NH_4^+-N adsorption [19].

3.2.3. Initial pH effect on NH_4^+-N adsorption

pH significantly affected the NH_4^+-N removal by biochar, as increasing pH increases the NH_4^+ adsorption capacity (Figure 4). The adsorption capacity was the lowest at pH 3 and were 0.98mg/g, 1.27mg/g, and 0.78mg/g for WB300, WB450 and WB600, respectively, and the highest at pH 9 were 1.56mg/g, 1.80mg/g, and 1.59mg/g, respectively. Ammonium adsorption did not reach the maximum for WB450 in the pH range 3-7. Below pH 7, a higher concentration of H^+ ions led to competition between NH_4^+ and H^+ for adsorption sites on the biochar surface, thereby reducing the adsorption of NH_4^+. As pH increased above 7, the H^+ concentration decreased, and more NH_4^+ ions were adsorbed [23]. When pH>7.5, the NH_4^+ ions can react with OH^- ions to form NH_3, causing the NH_4^+ concentration in the aqueous solution to decrease, thereby decreasing the amount of NH_4^+ adsorption [3]; the same effect was also observed by other researchers [18,49,58]. Thereby, a slightly alkaline solution will be the most suitable for NH_4^+ adsorption.

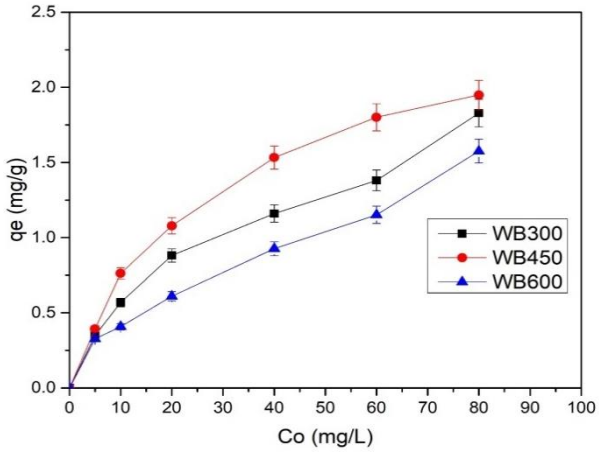

Fig. 2. Effect of initial NH_4^+-N concentration on adsorption (Experimental condition: Biochar dosage = 0.2g/L, Initial NH_4^+-N concentration = 60mL, pH=7±0.2, Speed = 200r/min, Temp.= 25ºC; Contact time=24h)

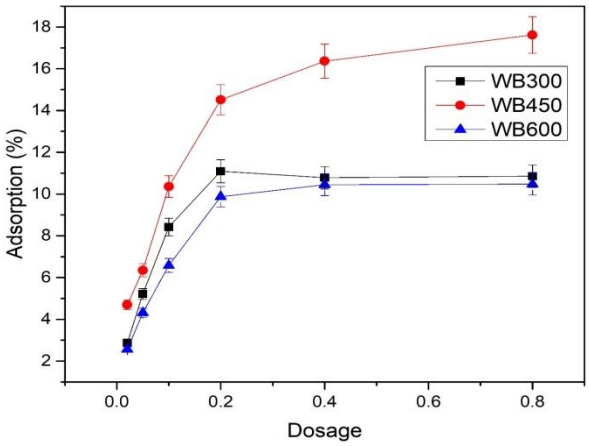

Fig. 3. Effect of biochar dosage on NH_4^+-N adsorption (Experimental condition: Initial NH_4^+-N concentration = 60mg/L, Temp. = 25ºC, pH = 7±0.2, Speed=200r/min.; Contact time=24h).

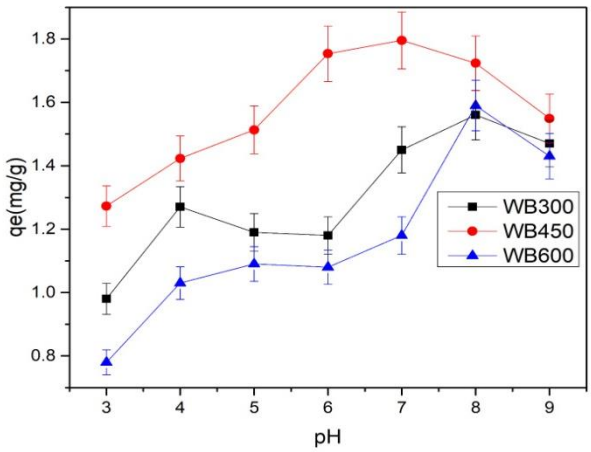

Fig. 4. The effect of initial solution pH on the NH_4^+-N adsorption; (Experimental condition: Biochar dosage, =0.2g/L; initial NH_4^+-N conc. =60mg/L, Temp.=25ºC; speed =200 r/min; Time=24h.).

3.2.4. Contact time effect on NH_4^+-N adsorption

The adsorption of NH_4^+-N rose significantly in the first 60 minutes and then slowed down for the next 180 minutes before finally plateauing. And this indicates 240 minutes of contact time is sufficient to achieve adsorption equilibrium. To begin with, fast ion uptake is a physical process that occurs primarily through mass transfer between solid and liquid phases, based on the ion concentration gradient [18,19,59]. As physical sorption comes to an end, the slower phase shows an ionic equilibrium between the solid and liquid phases, with some NH_4^+ ions slightly desorbing. Finally, chemisorption, which persists until the active sites are saturated, accounts for the slower and more steady increase [60,61]. Another research using zeolite has also shown a similar pattern [17]. Due to a different adsorbent, the equilibrium contact duration in that research is substantially shorter than in this study.

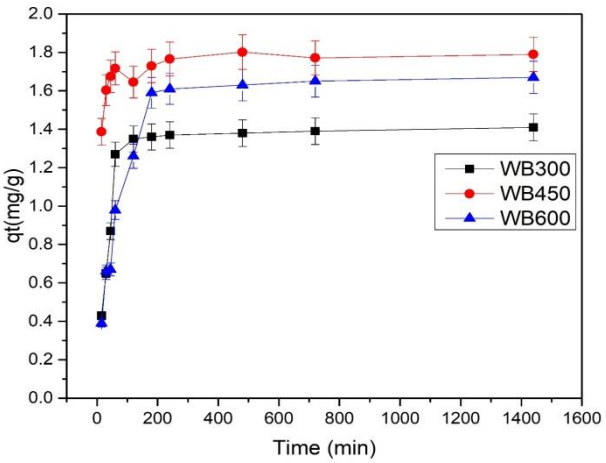

Fig. 5. Effect of contact time on NH_4^+-N adsorption; (Experimental condition; biochar dosage=0.2g/L; initial NH_4^+-N = 60mg/L, pH=7±0.2, Speed =200r/min. Temp.=25ºC; Time=24h).

3.3. Modeling of the NH_4^+-N adsorption data

3.3.1. Adsorption kinetics model

According to Table 3, the adsorption kinetics data of NH_4^+-N onto a WB450 dosage 0.2g in 60 mL of the initial 60mg/L NH_4^+-N solution was at room temperature 25ºC, a pH of 7, and a shaking speed of 200 r/min. These data were used to fit the kinetic models to describe the mechanism that NH_4^+-N adsorbed onto the wood biochar.

NH_4^+-N adsorption onto the wood biochar was defined by the 'pseudo-second-order' model based on the experimental results. The 'pseudo-second-order' model regression coefficient (R^2 = 0.999) was significantly higher than those of the pseudo-first-order model (R^2 = 0.296) based on the computed values in Table 3 and experimental data in (Table S4). As a result, "qe" values from the kinetic trials were in good agreement with the 'pseudo-second-order' model. The observed value of "qe" (1.8017mg/g) and the computed value of "qe" (1.795mg/g) differed immediately in the pseudo-second-order model. The actual result (1.8017mg/g) differed significantly from the estimated value (1.455mg/g) in the pseudo-first-order model. The pseudo-second-order kinetic model accurately predicted the NH_4^+-N adsorption on the wood biochar adsorbent. Chemisorption may be the dominant mode of NH_4^+-N adsorption on wood biochar, as demonstrated by earlier research with comparable results to this study and incorporated further analyses, such as FTIR, to reach this conclusion [20,23,59].

Table 3. Kinetic parameters for NH_4^+-N adsorption by wood biochar produced at 300ºC (WB300) and 450ºC (WB450) and to 600ºC (WB600) (pH = 7±0.2; biochar dosage = 0.2g/L).

	Pseudo-first-order model			Pseudo-second-order model		
WB450	**q_e (mg/g)**	**K_1 ($min^{-1}*10^{-3}$)**	**R^2**	**q_e (mg/g)**	**K_2 (g/mg/min)**	**R^2**
	1.455	0.305	0.296	1.795	0.118	0.999

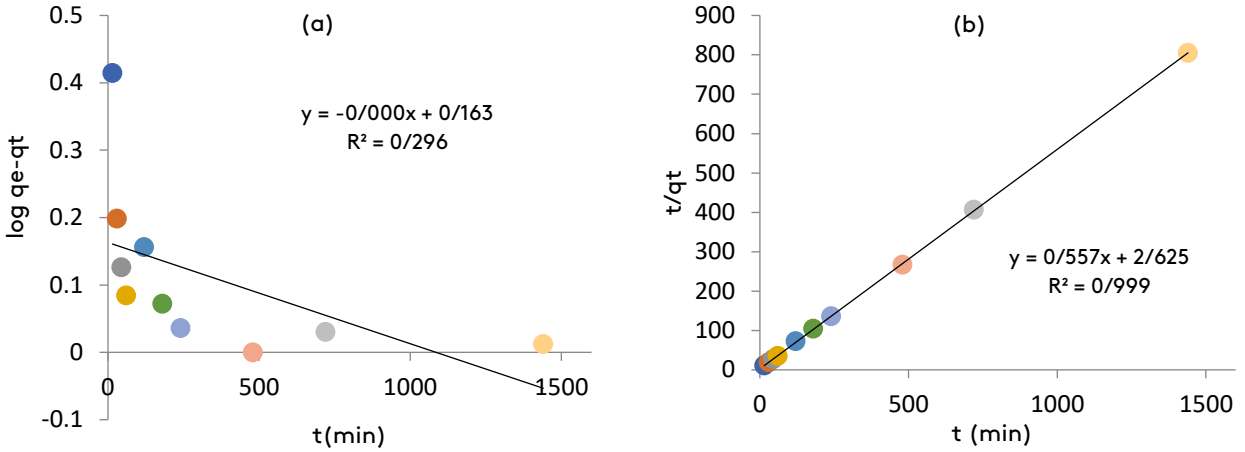

Fig. 6. Adsorption kinetic models; (a) Pseudo first order (b) Pseudo second order; pH= 7±0.2, biochar dosage = 0.2g/L, Speed = 200r/min, Temp.=25ºC.

3.3.2. Adsorption isotherm model

The adsorption isotherm was used to investigate the effects of the ammonium nitrogen concentrations of 20, 40, 60, and 80mg/L. The equilibrium adsorption processes of the WB300, WB450, and WB600 biochar were explained using two types of adsorption isotherm models. The Langmuir model's "R_L" values for all the biochars are between 0 and 1, which means the process was favorable. For the Freundlich model, the values of 1/n for all the biochar lie between 0 and 1, indicating favorability. Similar situations were reported in other studies of NH_4^+-N adsorption [22,62].

Table 4. Langmuir and Freundlich isotherm parameters for NH_4^+-N adsorption on WB300, WB450, and WB600 biochars

	Langmuir model				Freundlich model		
	q_o (mg/g)	b (L/mg)	R^2	R_L	1/n	K_f	R^2
WB300	2.151	0.0418	0.940	0.827	0.501	0.205	0.988
WB450	2.347	0.0653	0.996	0.754	0.486	0.270	0.964
WB600	1.980	0.0328	0.872	0.859	0.509	0.156	0.973

The adsorption data typically fit the Freundlich model with R^2> 0.96 compared to the Langmuir model in the regression coefficient (R^2). The Langmuir model based on monolayer sorption was preferred over the Freundlich model based on a heterogeneous surface. The Freundlich model has also been used to describe the adsorption features of NH_4^+-N in other investigations [20,22,62,63]. The "b" value (L/mg) in the Langmuir model and the "Kf" value in the Freundlich model were taken into consideration to compare the adsorption affinity of NH_4^+-N onto biochar WB300, WB450, and WB600. This indicates a stronger affinity for WB450 than WB300 and WB600 in terms of NH4$^+$-N adsorption; in both models, WB450 had the highest values. According to the "b" values and "Kf" values, the adsorption affinity trend of the biochar was WB450>WB300>WB600 (Table 4). Moreover, the maximum calculated adsorption capacity "qo" was 2.347mg/g on the WB450 biochar.

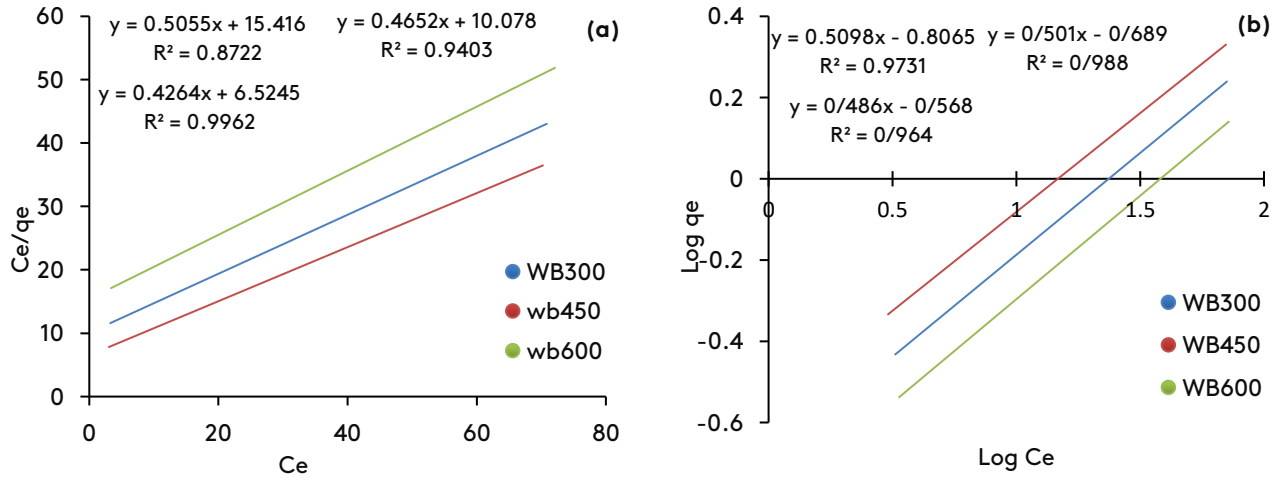

Fig. 7. Adsorption isotherm models (a) Langmuir model (b) Freundlich model; pH= 7±0.2, biochar dosage = 0.2g/L, shaking speed = 200r/min, Temp.= 25ºC).

3.4. Mechanisms of NH_4^+-N adsorption

The adsorption of NH_4^+-N using wood biochar may involve several adsorbent-adsorbate interactions, such as electrostatic attraction and chemical bonding. In this study, the adsorption process of NH_4^+N ions onto wood biochar was dominated by the heterogeneity surface with R^2>0.96 for all biochar based on Freundlich's model. WB450, which had the highest adsorption potential, was further examined to determine the process taking place during adsorption. The pseudo-second-order kinetic model fitted well with R^2=0.999, meaning that the chemisorption was probably dominating the adsorption process. Thus, chemical bonding and electrostatic interaction of NH_4^+-N with functional groups were likely the major mode of action. WB450 showed the highest NH_4^+-N adsorption capacity (2.34mg/g) and the highest "Kf" value (0.27) compared to other studies, as shown in Table 5. It was also found that the experimental "qe" of WB450 at an initial concentration of 40mg/L of NH_4^+-N was 1.53mg/g, which is higher than the qe of adsorbent reported by some previous literature at their higher initial concentrations, including natural Chinese clinoptilolite at 57.17mg/L with 0.951mg/g and sawdust at 50mg/L with 1.27mg/g [65,67]. This showed that WB450 also had higher adsorption potential than the other feedstock adsorbents. This illustrates that pyrolysis temperature and feedstock type affect NH4+ adsorption. The WB450 biochar may have retained more cellulose chains and lignin functional groups such as alcohols, acids, and hydroxides from its wood-derived feedstock (Abdolali et al. 2014). The surface complex formation with oxygen-containing groups such as carboxyl and carbonyl groups may also have enhanced NH_4^+ adsorption by the biochar (Cui et al. 2016). Further studies on the analysis of the different characteristics of the feedstock and how they may affect the NH_4^+ adsorption efficiency of biochar would be beneficial. The dominant mechanisms for NH_4^+ adsorption by the three biochar studied are likely chemical bonding and electrostatic interaction rather than physical adsorption.

Table 5. Maximum adsorption capacities (mg/g) of various adsorbents for NH_4^+-N.

Adsorbents'	Adsorption' rate (mg/g)	Reference
'Maple wood biochar'	0.46-0.87	[62]
'Giant reed biochar'	1.2-1.5	[64]
Sawdust	1.7	[65]
Posidonia oceanic Fibres	1.9	[66]
'Biochar made from Phragmites spp'.	2.2-5.4	[32]
Municipal Green waste wood biochar	2.347	In this study

4. Conclusions

Biochar WB300, WB450, and WB600 were pyrolyzed under slow pyrolysis and used to remove NH_4^+-N

from aqueous environments; their adsorption capabilities were modified by pyrolysis temperature, NH_4^+-N concentration, initial solution pH, and contact time. The pseudo-second-order model and the Freundlich isotherm model best-suited adsorption data from the biochar studied in this work. The adsorption on biochar is likely driven by the chemical bonding and polar interaction between NH_4^+-N and the surface's functional groups. Compared to WB300 and WB600, biochar WB450 had a better adsorption capacity. The highest "b" (L/mg), "qo" (mg/g), and "Kf" values were found for WB450, indicating greater adsorption affinity and capacity to bind. The maximum capacity of 2.34 mg/g NH_4^+-N removal was achieved at a pH of 7 and a contact time of 240 minutes. Thus, slow-pyrolysis may be used to produce biochar that can be used to remove water contaminants such as NH_4^+-N from the aqueous environment. Compared to other findings, the study concludes that biochar from green waste wood, a low-cost feedstock, can be considered a potential adsorbent for removing NH_4^+-N from an aqueous environment. And slow pyrolysis is a feasible environmental technology to develop biochar for the removal of water pollutants.

Acknowledgment

The authors would like to express their gratitude to the China Scholarship Council (CSC) for providing financial support to complete this study. We would like to thank anonymous reviewers for their assistance in refining the wording and conducting an in-depth conversation that aided in improving this work.

References

[1] Cui, X., Hao, H., Zhang, C., He, Z., Yang, X. (2016). Capacity and mechanisms of ammonium and cadmium sorption on different wetland-plant derived biochars. *Science of the total environment*, *539*, 566-75.

[2] Yang, P., Guo, D., Chen, Z., Cui, B., Xiao, B., Liu, S. (2017). Removal of Cr (VI) from aqueous solution using magnetic biochar synthesized by a single-step method. *Journal of dispersion science and technology, 38*(11), 1665-–74.

[3] Ismail, Z. Z., Hameed, B. B. (2014). A new application of giant reed waste material for ammonium removal. *International journal of environmental studies*, *71*(2), 122-138.

[4] Zhang, M., Wang, Z., Xu, J., Liu, Y., Ni, L., Cao, T., Xie, P. (2011). Ammonium, microcystins, and hypoxia of blooms in eutrophic water cause oxidative stress and C–N imbalance in submersed and floating-leaved aquatic plants in Lake Taihu, China. *Chemosphere*, *82*(3), 329-339.

[5] Richardson, S. D., DeMarini, D. M., Kogevinas, M., Fernandez, P., Marco, E., Lourencetti, C., Villanueva, C. M. (2010). What's in the pool? A comprehensive identification of disinfection by-products and assessment of mutagenicity of chlorinated and brominated swimming pool water. *Environmental health perspectives*, *118*(11), 1523-1530.

[6] Hafizur, R. M., Nuralam, H. M., Rumainul, I. M. (2017). Investigation of physicochemical parameter, heavy metal in Turag river water and adjacent industrial effluent in Bangladesh. *Journal of science, technology and environment informatics*, *5*(1), 347-360.

[7] Bhatnagar, A., Kumar, E., Sillanpää, M. (2010). Nitrate removal from water by nano-alumina: Characterization and sorption studies. *Chemical engineering journal*, *163*(3), 317-323.

[8] Ding, W. C., Zeng, X. L., Hu, X. B., Deng, Y., Hossain, M. N., Chen, L. (2018). Characterization of dissolved organic matter in mature leachate during ammonia stripping and two-stage aged-refuse bioreactor treatment. *Journal of environmental engineering*, *144*(1), 04017082.

[9] Moradzadeh, M., Moazed, H., Sayyad, G., Khaledian, M. (2014). Transport of nitrate and ammonium ions in a sandy loam soil treated with potassium zeolite–evaluating equilibrium and non-equilibrium equations. *Acta ecologica sinica*, *34*(6), 342-350.

[10] Samatya, S., Kabay, N., Yüksel, Ü., Arda, M., Yüksel, M. (2006). Removal of nitrate from aqueous solution by nitrate selective ion exchange resins. *Reactive and functional polymers*, *66*(11), 1206-1214.

[11] Hu, Q., Chen, N., Feng, C., Hu, W. (2015). Nitrate adsorption from aqueous solution using granular chitosan-Fe^{3+} complex. *Applied surface science*, *347*, 1-9.

[12] Schoeman, J. J., Steyn, A. (2003). Nitrate removal with reverse osmosis in a rural area in South Africa. *Desalination*, *155*(1), 15-26.

[13] Ahmad, M., Ahmad, M., Usman, A. R., Al-Faraj, A. S., Abduljabbar, A. S., Al-Wabel, M. I. (2018). Biochar composites with nano zerovalent iron and eggshell powder for nitrate removal from aqueous solution with coexisting chloride ions. *Environmental science and pollution research*, *25*(26), 25757-25771.

[14] Adeleye, A. S., Conway, J. R., Garner, K., Huang, Y., Su, Y., Keller, A. A. (2016). Engineered nanomaterials for water treatment and remediation: Costs, benefits, and applicability. *Chemical engineering journal*, *286*, 640-662.

[15] Tyagi, S., Rawtani, D., Khatri, N., Tharmavaram, M. (2018). Strategies for nitrate removal from aqueous environment using nanotechnology: a review. *Journal of water process engineering*, *21*, 84-95.

[16] Zhang, H., Xiao, R., Huang, H., Xiao, G. (2009). Comparison of non-catalytic and catalytic fast pyrolysis of corncob in a fluidized bed reactor. *Bioresource technology*, *100*(3), 1428-1434.

[17] Saltalı, K., Sarı, A., & Aydın, M. (2007). Removal of ammonium ion from aqueous solution by natural Turkish (Yıldızeli) zeolite for environmental quality. *Journal of hazardous materials*, *141*(1), 258-263.

[18] Halim, A. A., Latif, M. T., Ithnin, A. (2013). Ammonia removal from aqueous solution using organic acid modified activated carbon. *World applied sciences journal*, *24*(1), 1-6.

[19] Long, X. L., Cheng, H., Xin, Z. L., Xiao, W. D., Li, W., Yuan, W. K. (2008). Adsorption of ammonia on activated carbon from aqueous solutions. *Environmental progress*, *27*(2), 225-233.

[20] Zhao, Y., Yang, Y., Yang, S., Wang, Q., Feng, C., & Zhang, Z. (2013). Adsorption of high ammonium nitrogen from wastewater using a novel ceramic adsorbent and the evaluation of the ammonium-adsorbed-ceramic as fertilizer. *Journal of colloid and interface science*, *393*, 264-270.

[21] Sharifnia, S., Khadivi, M. A., Shojaeimehr, T., Shavisi, Y. (2016). Characterization, isotherm and kinetic studies for ammonium ion adsorption by light expanded clay aggregate (LECA). *Journal of saudi chemical society*, *20*, S342-S351.

[22] Tian, J., Miller, V., Chiu, P. C., Maresca, J. A., Guo, M., Imhoff, P. T. (2016). Nutrient release and ammonium sorption by poultry litter and wood biochars in stormwater treatment. *Science of the total environment*, *553*, 596-606.

[23] Kizito, S., Wu, S., Kirui, W. K., Lei, M., Lu, Q., Bah, H., Dong, R. (2015). Evaluation of slow pyrolyzed wood and rice husks biochar for adsorption of ammonium nitrogen from piggery manure anaerobic digestate slurry. *Science of the total environment*, *505*, 102-112.

[24] Yang, H. I., Lou, K., Rajapaksha, A. U., Ok, Y. S., Anyia, A. O., Chang, S. X. (2018). Adsorption of ammonium in aqueous solutions by pine sawdust and wheat straw biochars. *Environmental science and pollution research*, *25*(26), 25638-25647.

[25] Li, B., Yang, L., Wang, C. Q., Zhang, Q. P., Liu, Q. C., Li, Y. D., Xiao, R. (2017). Adsorption of Cd (II) from aqueous solutions by rape straw biochar derived from different modification processes. *Chemosphere*, *175*, 332-340.

[26] Tong, X. J., Li, J. Y., Yuan, J. H., Xu, R. K., Zhou, L. X. (2012). Adsorption of Cu (II) on rice straw char from acidic aqueous solutions. *Environmental. chemistry*, *31*(1), 64-68.

[27] Yargicoglu, E. N., Sadasivam, B. Y., Reddy, K. R., Spokas, K. (2015). Physical and chemical characterization of waste wood derived biochars. *Waste management*, *6*, 256-268.

[28] Cao, X., Ma, L., Gao, B., Harris, W. (2009). Dairy-manure derived biochar effectively sorbs lead and atrazine. *Environmental science and technology*, *43*(9), 3285-3291.

[29] Ahmad, M., Upamali, A., Eun, J., Zhang, M., Bolan, N. (2014). Biochar as a sorbent for contaminant management in soil and water: A review. *Chemosphere*, 99, 19-33.

[30] Tan, X., Liu, Y., Zeng, G., Wang, X., Hu, X., Gu, Y. (2015). Application of biochar for the removal of pollutants from aqueous solutions. *Chemosphere, 125*(10), 70-85.

[31] Takaya, C.A., Fletcher, L.A, Singh, S., Anyikude, K.U, Ross, A.B. (2016). Phosphate

and ammonium sorption capacity of biochar and hydrochar from different wastes. *Chemosphere*, *145*, 518-27.

[32] Zeng, Z., Zhang, S. D., Li, T. Q., Zhao, F. L., He, Z. L., Zhao, H. P., Rafiq, M. T. (2013). Sorption of ammonium and phosphate from aqueous solution by biochar derived from phytoremediation plants. *Journal of Zhejiang university science B*, *14*(12), 1152-1161.

[33] Hale, S.E., Alling, V., Martinsen, V., Mulder, J., Breedveld, G.D., Cornelissen, G. (2013). The sorption and desorption of Phosphate-P, Ammonium-N and Nitrate-N in cacao shell and corn cob biochars. *Chemosphere*, *91*(11), 1612–9.

[34] Yao, Y., Gao, B., Chen, J., Yang, L. (2013). Engineered biochar reclaiming phosphate from aqueous solutions: mechanisms and potential application as a slow-release fertilizer. *Environmental science and technology*, *47*(15), 8700-8708.

[35] Fornes, F., Belda, R. M., Lidón, A. (2015). Analysis of two biochars and one hydrochar from different feedstock: focus set on environmental, nutritional and horticultural considerations. *Journal of cleaner production*, *86*, 40-48.

[36] Xiang, J., Liu, D., Ding, W., Yuan, J., Lin, Y. (2015). Effects of biochar on nitrous oxide and nitric oxide emissions from paddy field during the wheat growth season. *Journal of cleaner production*, *104*, 52-58.

[37] Lou, K., Rajapaksha, A. U., Ok, Y. S., Chang, S. X. (2016). Pyrolysis temperature and steam activation effects on sorption of phosphate on pine sawdust biochars in aqueous solutions. *Chemical speciation and bioavailability*, *28*(1-4), 42-50.

[38] Rajapaksha, A. U., Chen, S. S., Tsang, D. C., Zhang, M., Vithanage, M., Mandal, S., Ok, Y. S. (2016). Engineered/designer biochar for contaminant removal/immobilization from soil and water: potential and implication of biochar modification. *Chemosphere*, *148*, 276-291.

[39] Mittal, A., Mittal, J., Malviya, A., Kaur, D., Gupta, V. K. (2010). Adsorption of hazardous dye crystal violet from wastewater by waste materials. *Journal of colloid and interface science*, *343*(2), 463-473.

[40] Foo, K. Y., Hameed, B. H. (2010). Insights into the modeling of adsorption isotherm systems. *Chemical engineering journal*, *156*(1), 2-10.

[41] Chen, X., Chen, G., Chen, L., Chen, Y., Lehmann, J., McBride, M. B., Hay, A. G. (2011). Adsorption of copper and zinc by biochars produced from pyrolysis of hardwood and corn straw in aqueous solution. *Bioresource technology*, *102*(19), 8877-8884.

[42] Silber, A., Levkovitch, I., Graber, E. R. (2010). pH-dependent mineral release and surface properties of cornstraw biochar: agronomic implications. *Environmental science and technology*, *44*(24), 9318-9323.

[43] Chun, Y., Sheng, G., Chiou, C. T., Xing, B. (2004). Compositions and sorptive properties of crop residue-derived chars. *Environmental science and technology*, *38*(17), 4649-4655.

[44] Harvey, O. R., Herbert, B. E., Kuo, L. J., Louchouarn, P. (2012). Generalized two-dimensional perturbation correlation infrared spectroscopy reveals mechanisms for the development of surface charge and recalcitrance in plant-derived biochars. *Environmental science and technology*, *46*(19), 10641-10650.

[45] Spokas, K. A. (2010). Review of the stability of biochar in soils: predictability of O: C molar ratios. *Carbon management*, *1*(2), 289-303.

[46] Thangalazhy-Gopakumar, S., Adhikari, S., Ravindran, H., Gupta, R. B., Fasina, O., Tu, M., Fernando, S. D. (2010). Physiochemical properties of bio-oil produced at various temperatures from pine wood using an auger reactor. *Bioresource technology*, *101*(21), 8389-8395.

[47] Williams, P. T., Nugranad, N. (2000). Comparison of products from the pyrolysis and catalytic pyrolysis of rice husks. *Energy*, *25*(6), 493-513.

[48] Shabangu, S., Woolf, D., Fisher, E. M., Angenent, L. T., Lehmann, J. (2014). Techno-economic assessment of biomass slow pyrolysis into different biochar and methanol concepts. *Fuel*, *117*, 742-748.

[49] Aysu, T., Küçük, M.M. (2014). Biomass pyrolysis in a fixed-bed reactor: Effects of

pyrolysis parameters on product yields and characterization of products. *Energy*, 64, 1002–25.

[50] Méndez, A., Tarquis, A.M., Saa-Requejo, A., Guerrero, F., Gascó, G. (2013). Influence of pyrolysis temperature on composted sewage sludge biochar priming effect in a loamy soil. *Chemosphere*, 93(4), 668–76.

[51] Yuan, H., Lu, T., Wang, Y., Huang, H., Chen, Y. (2014). Influence of pyrolysis temperature and holding time on properties of biochar derived from medicinal herb (radix isatidis) residue and its effect on soil CO_2 emission. *Journal of analytical and applied pyrolysis*, *110*, 277-284.

[52] Li, M., Huang, H., Yu, S., Tian, N., Dong, F., Du, X., Zhang, Y. (2016). Simultaneously promoting charge separation and photoabsorption of BiOX (X= Cl, Br) for efficient visible-light photocatalysis and photosensitization by compositing low-cost biochar. *Applied surface science*, *386*, 285-295.

[53] Gai, X., Wang, H., Liu, J., Zhai, L., Liu, S., Ren, T., Liu, H. (2014). Effects of feedstock and pyrolysis temperature on biochar adsorption of ammonium and nitrate. *PloS one*, *9*(12), e113888.

[54] Crombie, K., Mašek, O. (2014). Investigating the potential for a self-sustaining slow pyrolysis system under varying operating conditions. *Bioresource technology*, *162*, 148-156.

[55] Song, W., Guo, M. (2012). Quality variations of poultry litter biochar generated at different pyrolysis temperatures. *Journal of analytical and applied pyrolysis*, *94*, 138-145.

[56] Sica, M., Duta, A., Teodosiu. C., Draghici, C. (2014). Thermodynamic and kinetic study on ammonium removal from a synthetic water solution using ion exchange resin. *Clean technologies environmental policy*, *16*(2), 351–359.

[57] Huang, H., Xiao, X., Yan, B., Yang, L. (2010). Ammonium removal from aqueous solutions by using natural Chinese (Chende) zeolite as adsorbent. *Journal of hazardous materials*, *175*(1-3), 247-252.

[58] Kong, Y., Wang, Z.L., Wang, Y., Yuan, J., Chen, Z.D. (2011). Degradation of methyl orange in artificial wastewater through electrochemical oxidation using exfoliated graphite electrode. *Xinxing tan cailiao/new carbon mater*, *26*(6), 459-64.

[59] Zhu, K., Fu, H., Zhang, J., Lv, X., Tang, J., Xu, X. (2012). Studies on removing NH4+-N from aqueous solution by using the activated carbons derived from rice husk. *Biomass and bioenergy*, *43*, 18-25.

[60] Kučić, D., Ćosić, I., Vuković, M., Briški, F. (2013). Sorption kinetic studies of ammonium from aqueous solution on different inorganic and organic media. *Acta chimica slovenica*, *60*(1), 109-119.

[61] Baocheng, Q. U., Jiti, Z. H. O. U., Xiang, X., Zheng, C., Hongxia, Z. H. A. O., Xiaobai, Z. H. O. U. (2008). Adsorption behavior of Azo Dye CI Acid Red 14 in aqueous solution on surface soils. *Journal of environmental sciences*, *20*(6), 704-709.

[62] Wang, B., Lehmann, J., Hanley, K., Hestrin, R., Enders, A. (2015). Adsorption and desorption of ammonium by maple wood biochar as a function of oxidation and pH. *Chemosphere*, *138*, 120-6.

[63] Liu, N., Sun, Z. T., Wu, Z. C., Zhan, X. M., Zhang, K., Zhao, E. F., Han, X. R. (2013). Adsorption characteristics of ammonium nitrogen by biochar from diverse origins in water. In *advanced materials research 664*, 305-312.

[64] Hou, J., Huang, L., Yang, Z., Zhao, Y., Deng, C., Chen, Y., Li, X. (2016). Adsorption of ammonium on biochar prepared from giant reed. *Environmental science and pollution research*, *23*(19), 19107-19115.

[65] Wahab, M. A., Jellali, S., Jedidi, N. (2010). Ammonium biosorption onto sawdust: FTIR analysis, kinetics and adsorption isotherms modeling. *Bioresource technology*, *101*(14), 5070-5075.

[66] Jellali, S., Wahab, M.A., Anane, M., Riahi, K., Jedidi, N. (2010). Biosorption characteristics of ammonium from aqueous solutions onto Posidonia oceanica (L.) fibres. *Desalination*, *270*(1–3), 40-9.

[67] Wang, M., Liao, L., Zhang, X., Li, Z., Xia, Z., Cao, W. (2011). Adsorption of low-concentration ammonium onto vermiculite

from Hebei province, China. *Clays clay miner, 59*(5), 459-65.

[68] Cui, X., Hao, H., Zhang, C., He, Z., Yang, X. (2016). Capacity and mechanisms of ammonium and cadmium sorption on different wetland-plant derived biochars. *Science of the total environment*, *539*, 566-575.

[69] Abdolali, A., Guo, W. S., Ngo, H. H., Chen, S. S., Nguyen, N. C., Tung, K. L. (2014). Typical lignocellulosic wastes and by-products for biosorption process in water and wastewater treatment: a critical review. *Bioresource technology*, *160*, 57-66.